Adv. Studies Theor. Phys., Vol. 2, 2008, no. 5, 243 - 260

Steady Creeping Motion of a Liquid Bubble in an Immiscible Viscous Fluid Bounded by a Vertical Porous Cylinder of Finite Thickness[1]

Nirmal C. Sacheti and Pallath Chandran [2]

Department of Mathematics and Statistics
College of Science, Sultan Qaboos University
PC 123, Al Khod, Muscat, Sultanate of Oman

Bal S. Bhatt

Department of Mathematics and Computer Science
The University of West Indies, Trinidad, West Indies

Raj P. Chhabra

Department of Chemical Engineering
Indian Institute of Technology, Kanpur-208 016, India

Abstract

The creeping vertical motion of a fluid sphere (drop or gas) or liquid bubbles of different shapes in another immiscible fluid confined by porous boundaries is encountered in several situations in industry and technology. Such flows are generally multi-phase in nature. In this work, we have considered a flow field comprising a non-Newtonian bubble region surrounded by a liquid film of Newtonian fluid. This inner region is bounded by a permeable cylindrical medium pervaded by the same Newtonian fluid. We have studied the interaction features of this multi-phase flow in terms of certain practically important geometrical and physical parameters. We have carried out an exact analysis of the governing equations in the three flow fields — Non-Newtonian, Newtonian

[1]This work was supported by the Sultan Qaboos University Research Grant No. IG/SCI/DOMS/06/08.

[2]chandran@squ.edu.om

film and porous regions. The effects of pressure gradient, permeability and rheological parameters on the bubble velocity and the flow in different regions have been discussed.

Keywords: micropolar liquid bubble, immiscible fluid, creeping motion, bubble velocity, pressure gradient, porous medium, permeability, rheological parameters.

1 Introduction

The theoretical and experimental studies of laminar motion of bubbles, drops and spherical as well as non-spherical particles in different fluid media have been a subject of exhaustive investigations in the literature (see, for instance, [10–13, 16–18]) for several decades. Such studies have received attention of a large number of scientists for both academic and practical interests, mainly due to large number of applications in diverse fields. For example, it is well known that a good understanding of the behaviour of a rising bubble in polymeric solutions can be of great help in areas such as volcanic eruptions, decompression sickness, glass manufacturing, wastewater treatment, fermentation, metallurgical processes, to name a few. On the other hand, a sound knowledge of the movement of a single liquid drop in another immiscible liquid, e.g., a Newtonian fluid drop in another Newtonian fluid medium, a power law fluid (non-Newtonian) drop in a Newtonian liquid, etc., may well represent an idealization of many industrially key processes such as atomization, food processing, liquid-liquid extraction, production of polymer blends and emulsions in the paint and detergent industries [19].

The study of stratified flow of two immiscible fluids in the presence of porous boundaries is another important area of investigation as it can also indicate idealization of several engineering processes and applications such as manufacture of foam plastics, degradation of polymer melts in membrane modules in polymer processing, controlled release applications encountered in pharmaceutical and agricultural engineering processes, oxygenation of blood encountered in physiological flows, etc. For instance, in petroleum engineering, during the application of steam-injection method for enhanced oil recovery, water and oil (as droplets) flow simultaneously through the porous rocks. Similarly, in the accidental spills of multi-phase systems (oil and water) and the discharge of industrial effluents containing immiscible liquids into settling ponds, the two phases tend to stratify and flow along the porous walls of ponds. Therefore, in order to develop a rational understanding it is desirable to improve the design

of such processes and/or to ascertain the extent of environmental damage in terms of contamination of soils. Admittedly, the process here is quite complex due to the coupling of convection and diffusion of contaminants, thermal effects, etc. The same also applies to various other processes described earlier. Thus, a satisfactory understanding of the fluid mechanical aspects of the flow of two immiscible fluids in the presence of bounding porous media is germane to the modeling of the overall process involving simultaneous mass transport of a species. However, it is always desirable to build up the level of complexity in a gradual manner as seemingly simple flows with limited applicability, frequently, provide useful insights to develop more realistic models.

The study of slow movement of a single large liquid bubble, under gravity and laminar flow conditions, in a surrounding immiscible liquid has attracted the attention of researchers in the last few decades. In this direction, Goldsmith and Mason [7, 8] carried out comprehensive investigations involving both experimental and theoretical aspects and relating their work to real life applications such as flow of emulsions through narrow capillaries, deformation of red blood cells during the flow through the capillary system of the body, etc. They [7] assumed that a single large Newtonian fluid bubble, surrounded by an immiscible Newtonian fluid, was slowly translating in a narrow, infinite, vertical rigid circular tube. It was further assumed that the diameter of the tube was much smaller than the dimension of the undistorted bubble. They considered the cases of bubble rising as well as falling, under creeping flow condition for the flow. The solution of the governing equations for both phases, namely, inside region of bubble and the surrounding liquid, was obtained by solving simultaneously the corresponding equations for each region and then using an appropriate set of matching and boundary conditions. The theoretical counterpart of their work was later modified by Ravindran [14] to account for non-Newtonian (micropolar) features of the bubble. Subsequently, Bhatt [2] extended the work of Ravindran by considering a circular tube bounded by a porous medium. He argued that such a flow configuration, in which there is a surrounding porous medium, can be a more realistic model for the motion of red cells surrounded by plasma in a capillary of the human body. Bhatt [2] used Darcy law and the well-known Beavers-Joseph boundary condition [1] to model the flow in the porous medium and the interface condition, respectively. The work reported in [9] gives a good account of boundary conditions for Darcy's flow.

In many applications, the porous medium surrounding the tube will be not only of finite thickness, but may also be of moderate to high permeability. In

such cases, it is imperative to consider other equations to model the simultaneous flow in the surrounding porous medium. An appropriate porous medium model, extensively used in the literature in such cases, is the Brinkman equation (see [4, 5, 11]). As is known, the use of Brinkman equation necessitates considering a different set of matching conditions at the clear fluid-porous medium interface as well as no-slip conditions at the solid boundary [3, 15]. In this work, we have extended the work of Bhatt [2] by considering Brinkman equation. The use of this equation has led to our considering simultaneous flow in three regions: the non-Newtonian bubble region, the Newtonian film region and, additionally, a porous region of finite thickness. As a consequence, we need to use two sets of interface conditions: at the bubble-film interface and at the film-porous medium interface. Our main aim in this work is to investigate the effects of pressure gradient, permeability of the porous medium and the non-Newtonian parameters on key physical quantities such as the bubble velocity, and the fluid velocity in the porous medium as well as the entire region.

2 Governing Equations

We use the cylindrical polar coordinates (r, θ, z) with the positive z-axis as the downward vertical. Let the suffixes 1, 2, and 3 — used with the velocity (q) and the pressure (p) — denote the quantities associated with the bubble, the surrounding film and the porous medium, respectively. We denote the thickness of the film by h_1 and the thickness of the porous medium by h_2 . For the uni-directional flow in the z-direction being considered here, the vertical velocity components in the three regions are denoted by $q_i(r)$, $(i = 1, 2, 3)$. Let $\omega(r)$ be the micro-rotation associated with the micropolar fluid bubble.

As stated earlier, the momentum equations of a viscous, incompressible flow in a rigid tube were originally derived and discussed by Goldsmith & Mason [7]. For the present problem, the governing equations for the axisymmetric creeping flow in the three regions are given by [2, 6, 20]

Region I – Micropolar fluid flow: $0 \leq r \leq a - h_1$

$$(m_1 + m_2)\left(r\frac{d^2q_1}{dr^2} + \frac{dq_1}{dr}\right) + m_2\left(r\frac{d^2\omega}{dr^2} + \frac{d\omega}{dr}\right) - r\left(\frac{dp_1}{dz} - \rho_1 g\right) = 0 \tag{1}$$

$$m_3\left(r\frac{d^2\omega}{dr^2}+\frac{d\omega}{dr}-\frac{\omega}{r}\right)-m_2 r\left(\frac{dq_1}{dr}+2\omega\right)=0 \tag{2}$$

Region II – Newtonian film region: $a-h_1\le r\le a$

$$\mu\left(r\frac{d^2q_2}{dr^2}+\frac{dq_2}{dr}\right)-r\left(\frac{dp_2}{dz}-\rho_2 g\right)=0 \tag{3}$$

$$p_1(z)-p_2(z)=\frac{\beta}{a-h_1} \tag{4}$$

Region III – Porous medium (Brinkman model): $a\le r\le a+h_2$

$$\mu\left(r\frac{d^2q_3}{dr^2}+\frac{dq_3}{dr}\right)-r\left(\frac{dp_3}{dz}-\rho_2 g+\frac{\mu}{k}q_3\right)=0 \tag{5}$$

$$\frac{dp_1}{dz}=\frac{dp_2}{dz}=\frac{dp_3}{dz}=P,\ \text{a constant} \tag{6}$$

It may be mentioned that equation (4) follows from the Laplace capillary equation for the pressure distribution at the bubble/film interface [7].

In the above, m_1, m_2, m_3 are the micropolar parameters of the fluid in the bubble, p_i is the pressure, ρ_1 the density of the micropolar fluid, ρ_2 the density of the fluid occupying the film and the porous region, μ the viscosity of the fluid in regions II and III, β the interfacial tension in the bubble, a the radius of the tube, and k is the permeability of the porous medium.

3 Boundary and Interface Conditions

The equations (1), (2), (3) and (5) need to be solved subject to a set of boundary and matching conditions. Physically, these conditions can be described as

- Microrotation vanishes at the bubble/film interface
- q_1 and ω are finite on the axis ($r=0$)
- Velocities at the bubble–film interface ($r=a-h_1$) and at the film–porous medium interface ($r=a$) are continuous
- Shear stresses at the bubble–film interface ($r=a-h_1$) and film–porous medium interface ($r=a$) are continuous

- The flow is subject to the no-slip condition at $r = a + h_2$

In mathematical terms, the above conditions, together with the continuity of volume flux condition, can be written as

$$
\begin{aligned}
&\text{(a)} \quad \omega = 0 \ \text{ at } \ r = a - h_1 \\
&\text{(b)} \quad q_1 \ \text{ and } \ \omega \ \text{ are finite at } \ r = 0 \\
&\text{(c)} \quad q_1 = q_2 \ \text{ at } \ r = a - h_1 \\
&\text{(d)} \quad (m_1 + m_2)\frac{dq_1}{dr} = \mu \frac{dq_2}{dr} \ \text{ at } \ r = a - h_1 \\
&\text{(e)} \quad q_2 = q_3\,, \ \ \frac{dq_2}{dr} = \frac{dq_3}{dr} \ \text{ at } \ r = a \\
&\text{(f)} \quad q_3 = 0 \ \text{ at } \ r = a + h_2\,, \ \ h_2 = \epsilon_1 h_1\,, \ \ 0 < \epsilon_1 \leq 1 \\
&\text{(g)} \quad \int_0^{a-h_1} 2\pi r q_1(r)\, \mathrm{d}r = -\int_{a-h_1}^{a} 2\pi r q_2(r)\, \mathrm{d}r = \pi(a-h_1)^2 W
\end{aligned} \tag{7}
$$

In equation (7g), W is the bubble velocity, and all other quantities are as defined before. We also note that the condition (7g) above is physically more realistic than the one used in a related work [16].

4 Solution Procedure

We now proceed to obtain solutions of the governing equations in the three regions I—III using the relevant conditions given in equation (7). We shall first obtain an equation governing the microrotation ω. It may be noted that equation (2) is coupled with equation (1). Eliminating q_1 between equations (1) and (2), it can be shown that the differential equation of ω is

$$
r^2 \frac{d^2\omega}{dr^2} + r\frac{d\omega}{dr} - (\alpha^2 r^2 + 1)\omega = \frac{\alpha^2(P - g\rho_1)}{4m_1 + 2m_2} r^3 + \frac{C_1 \alpha^2}{2m_1 + m_2} r \tag{8}
$$

where C_1 is an arbitrary constant and $\alpha^2 = \frac{m_2(2m_1+m_2)}{m_3(m_1+m_2)}$.

Equation (8) can easily be re-written as a non-homogeneous Bessel equation of order 1, in the form

$$
x^2 \frac{d^2\omega}{dx^2} + x\frac{d\omega}{dx} - (x^2 + 1)\omega = F(x) \tag{9}
$$

where

$$
F(x) = \left(\frac{P - g\rho_1}{2\alpha(2m_1 + m_2)}\right) x^3 + \left(\frac{C_1 \alpha}{2m_1 + m_2}\right) x, \quad x = \alpha r
$$

The general solution of equation (8), expressed in terms of the original variable r, is

$$\omega(r) = C_2 I_1(\alpha r) + C_3 K_1(\alpha r) - \left(\frac{P - g\rho_1}{4m_1 + 2m_2}\right) r - \frac{C_1}{(2m_1 + m_2)r} \tag{10}$$

In the above, I_1 and K_1 denote the Bessel functions of first and second kind, respectively, each of order 1; and C_2 , C_3 are arbitrary constants, to be determined.

Having obtained the general solution for $\omega(r)$, we can now obtain an expression for $q_1(r)$ from equation (1), in the form

$$\begin{aligned} q_1(r) =& \frac{m_2}{\alpha(m_1 + m_2)} \left[-C_2 I_0(\alpha r) + C_3 K_0(\alpha r)\right] \\ &+ \left(\frac{P - g\rho_1}{4m_1 + 2m_2}\right) r^2 + \left(\frac{2C_1}{2m_1 + m_2}\right) \ln r + C_4 \,, \end{aligned} \tag{11}$$

C_4 being another constant of integration. Furthermore, I_0 and K_0 are modified Bessel functions of first and second kind, respectively, each of order 0 . This completes the solution for the bubble region.

The process of finding the general solution for the Region II is straightforward. Integration of equation (3) leads to

$$q_2(r) = \left(\frac{P - g\rho_2}{4\mu}\right) r^2 + C_5 \ln r + C_6 \tag{12}$$

C_5 and C_6 being another set of arbitrary constants.

We shall now obtain the solution of equation (5) valid in the porous region III. This equation can be first expressed as

$$r^2 \frac{d^2 q_3}{dr^2} + r \frac{dq_3}{dr} - \frac{r^2}{k} q_3 = \left(\frac{P - g\rho_2}{\mu}\right) r^2 \tag{13}$$

Following the same procedure as in the solution of the microrotation equation (8), one can show that equation (13) too transforms to a non-homogeneous Bessel equation of order zero, whose solution can be shown to be given by

$$q_3(r) = C_7 I_0\left(\frac{r}{\sqrt{k}}\right) + C_8 K_0\left(\frac{r}{\sqrt{k}}\right) - \frac{k(P - g\rho_2)}{\mu} \tag{14}$$

where C_7 and C_8 are arbitrary constants.

Equations (10), (11), (12) and (14) represent, respectively, the general solutions of the microrotation of the bubble in region I and the fluid velocity in the three regions of the flow. The particular solution for the problem at

hand can be obtained by evaluating the constants C_1–C_8 using the conditions in equation (7). It can be shown that these constants are given by

$$
\begin{aligned}
C_1 &= 0 \\
C_2 &= \frac{0.5(P - g\rho_1)(a - h_1)}{(2m_1 + m_2)I_1(\alpha a - \alpha h_1)} \\
C_3 &= 0 \\
C_4 &= \left(\frac{P - g\rho_2}{4\mu}\right) T_1 + \left(\frac{P - g\rho_1}{4m_1 + 2m_2}\right) T_2 \\
&\quad - \frac{g(\rho_1 - \rho_2)(a - h_1)^2 \ln(1 - h_1/a)}{2\mu} \\
C_5 &= \frac{g(\rho_2 - \rho_1)(a - h_1)^2}{2\mu} \\
C_6 &= \left[\frac{k(P - g\rho_2)}{4\mu}\right] T_3 + \frac{g(\rho_1 - \rho_2)(a - h_1)^2 \ln a}{2\mu} \\
C_7 &= \left[\frac{k(P - g\rho_2)}{2\mu}\right] T_4 \\
C_8 &= \left[\frac{k(P - g\rho_2)}{2\mu}\right] T_5
\end{aligned}
$$

In the above, the quantities T_1–T_5 are defined as

$$
\begin{aligned}
T_1 &= h_1^2 - 2ah_1 - 4k + k\left[2T_4 I_0\left(\frac{a}{\sqrt{k}}\right) + 2T_5 K_0\left(\frac{a}{\sqrt{k}}\right)\right] \\
T_2 &= \frac{m_2(a - h_1)}{\alpha(m_1 + m_2)} \frac{I_0(\alpha a - \alpha h_1)}{I_1(\alpha a - \alpha h_1)} - (a - h_1)^2 \\
T_3 &= 2T_4 I_0\left(\frac{a}{\sqrt{k}}\right) + 2T_5 K_0\left(\frac{a}{\sqrt{k}}\right) - \frac{a^2}{k} - 4 \\
T_4 &= \frac{1}{T_6}\left[2K_1\left(\frac{a}{\sqrt{k}}\right) + \left(\frac{\gamma a}{\sqrt{k}}\right) K_0\left(\frac{a + h_2}{\sqrt{k}}\right)\right] \\
T_5 &= \frac{1}{T_6}\left[2I_1\left(\frac{a}{\sqrt{k}}\right) - \left(\frac{\gamma a}{\sqrt{k}}\right) I_0\left(\frac{a + h_2}{\sqrt{k}}\right)\right]
\end{aligned}
$$

where

$$
\begin{aligned}
\gamma &= 1 - \frac{g(\rho_1 - \rho_2)(a - h_1)^2}{(P - g\rho_2)a^2} \\
T_6 &= I_0\left(\frac{a + h_2}{\sqrt{k}}\right) K_1\left(\frac{a}{\sqrt{k}}\right) + I_1\left(\frac{a}{\sqrt{k}}\right) K_0\left(\frac{a + h_2}{\sqrt{k}}\right)
\end{aligned}
$$

5 Bubble velocity

In this section, we shall obtain an analytical expression for the translation velocity of the bubble. Needless to say, in applications involving the flows of the type considered here, estimation of the bubble velocity and its variation with quantities such as pressure gradient, is of great practical importance.

To obtain the bubble velocity, we first consider the volumetric flux condition — *i. e.*, the continuity requirement for the flow — given in part (g) of equation (7), which is equivalent to two equations. One of these equations, namely,

$$\int_0^{a-h_1} 2\pi r q_1(r)\, \mathrm{d}r = \pi(a-h_1)^2 W \tag{15}$$

can be easily shown to give, after detailed algebra, an expression for the bubble velocity W, which would also include the pressure gradient P. On the other hand, the second equation, namely,

$$-\int_{a-h_1}^{a} 2\pi r q_2(r)\, \mathrm{d}r = \pi(a-h_1)^2 W\,, \tag{16}$$

in conjuction with the expression obtained for W earlier, using equation (15), can finally be shown to yield

$$(1-\alpha_1+2\lambda L+\lambda T_7)\,P-(1-\alpha_1+2\lambda L)g\rho_1-\lambda g\rho_2 T_7=0 \tag{17}$$

where

$$L=\frac{2ah_1-h_1^2}{(a-h_1)^2}$$

$$\lambda=\frac{2m_1+m_2}{2\mu}$$

$$\alpha_1=\frac{2m_2}{\alpha^2(m_1+m_2)(a-h_1)^2}\left[\alpha(a-h_1)\frac{I_0(\alpha a-\alpha h_1)}{I_1(\alpha a-\alpha h_1)}-2\right]$$

$$T_7=L^2-\frac{4k(L+1)^2}{a^2}\left[T_4 I_0\left(\frac{a}{\sqrt{k}}\right)+T_5 K_0\left(\frac{a}{\sqrt{k}}\right)-2\right]$$

As our emphasis in this work is on analysing the effects of pressure gradient and other parameters on W and q_3, we have not computed P. However, an explicit expression for P can be obtained, after some algebra, from equation (17) in conjuction with the expressions of T_4 and T_5.

Finally, an expression for the bubble velocity W can be obtained in the form

$$W=W_1+W_2+W_3+W_4+W_5 \tag{18}$$

where

$$W_1 = \frac{(P - g\rho_1)(a - h_1)^2}{8m_1 + 4m_2}$$

$$W_2 = \frac{m_2(g\rho_1 - P)}{(m_1 + m_2)(2m_1 + m_2)\alpha^2}$$

$$W_3 = \left(\frac{P - g\rho_2}{4\mu}\right)\left[h_1^2 - 2ah_1 - 4k + 2k\left\{T_4 I_0\left(\frac{a}{\sqrt{k}}\right) + T_5 K_0\left(\frac{a}{\sqrt{k}}\right)\right\}\right]$$

$$W_4 = \frac{g(\rho_2 - \rho_1)(a - h_1)^2 \ln(1 - h_1/a)}{2\mu}$$

$$W_5 = \left(\frac{P - g\rho_1}{4m_1 + 2m_2}\right)\left[\frac{m_2(a - h_1)}{\alpha(m_1 + m_2)}\,\frac{I_0(\alpha a - \alpha h_1)}{I_1(\alpha a - \alpha h_1)} - (a - h_1)^2\right]$$

6 Results

In this section, we shall analyze the effect of certain parameters (e.g., rheological, permeability of the porous medium) on some flow variables of practical interest. Our emphasis will be mainly on exhibiting plots of variation of the bubble velocity, W, and the velocity of fluid in the porous region ($0.4 \leq r \leq 0.5$). For the sake of completeness, we have also included a couple of graphs showing the variation of fluid velocity in all three regions of the cylinder, at a typical cross-section of the circular tube ($0 \leq r \leq 0.5$). It is to be mentioned that we have included two important cases, namely, $\rho_1 < \rho_2$ and $\rho_1 > \rho_2$, for each specific type of variation considered in this work. Both these cases are worthy of consideration from the view point of practical applications. In all figures presented in this section, we have taken the values of the parameters of which the effects of variations are not sought, as fixed constants: $g = 980$ cm s^{-2}, $a = 0.4$ cm, $k/a^2 = 0.2$, $\rho_1 = 0.5$ g cm^{-3}, $\rho_2 = 1.0$ g cm^{-3} (or, vice versa, depending on whether the bubble is falling or rising), $m_1/m_2 = 2$, $\mu = 1.3$ g cm^{-1} s^{-1}, $h_1 = h_2 = 0.1$ cm, and $\alpha = 5$ cm^{-1}.

In certain applications involving bubble motion in a surrounding fluid medium, it is desirable to determine the influence of the pressure gradient on the bubble velocity. Accordingly, in the Figures 1 through 4, we have investigated the variation of the bubble velocity (W) against the pressure gradient (P) by considering the effect of permeability (Figs 1 and 2) and of non-Newtonian parameters (Figs 3 and 4). As explained above, we have considered both the cases — Case I: $\rho_1 < \rho_2$ (Figs 1 and 3) and Case II: $\rho_1 > \rho_2$ (Figs 2 and 4).

In the Fig 1, the plots of variation of W versus P, for the case I, have been shown for two typical values of the permeability k of the porous medium.

Here, the bubble can be seen to rise for the range of values of P considered, and its velocity varies linearly with P. Barring relatively smaller values of P, the effect of the increase of the permeability of the porous medium is to enhance the bubble speed. However, the Figure 2, interestingly, presents a mixed scenario of the bubble motion for the case II. Here, the bubble can be seen to have downward motion (*i.e.*, a falling bubble) for smaller values of P ($\approx$ until 780) and then, for higher values of P, it shows upward motion. The effect of the permeability of the porous medium is, however, more or less similar to that observed for the case I (see the profiles in Fig 1). In the next set of figures, Figs 3 and 4, we have considered the effect of micropolar parameters m_1 and m_2 on W versus P plots by considering two specific values of the ratio m_2/m_1. In the case I (*i.e.*, $\rho_1 < \rho_2$), we notice that an increase in the value of this ratio results in the reduction in the magnitude of bubble velocity, especially for higher values of the pressure gradient. The bubble velocity profiles for the case II (*i.e.*, $\rho_1 > \rho_2$), resemble the ones shown in Fig 2. However, the effect of increase in micropolar parameters' ratio (see Fig 4) is generally insignificant, particularly when P values are close to 900 and beyond. Nevertheless, compared to the Fig 3 plots, the effect of the increase of this ratio on W, howsoever small, is opposite in nature.

The consideration of the Brinkman equation, as against Darcy's equation to model the flow [2] in the surrounding porous medium ($0.4 \leq r \leq 0.5$) has given rise to a variable velocity q_3 in the porous medium region. In Figs 5 and 6, the variation of q_3 with r (the radial coordinate) has been illustrated for the case I ($\rho_1 < \rho_2$) and case II ($\rho_1 > \rho_2$), respectively, for a range of values of the pressure gradient ($700 \leq P \leq 1000$). One can notice (Fig 5) that velocity plots for relatively higher values of P (≈ 900 or more) show upward motion of fluid in the entire region of the porous medium. However, for relatively smaller value of P ($\approx$ 700), the nature of flow in the porous region reverses, meaning there is now downward motion. From the physical point of view, this change in nature of flow can partly be attributed to opposing nature of the effects of gravity and applied pressure gradient on the overall flow. The plots of the q_3 velocity profiles in Fig 6, related to the case II, are similar, save for the change in concavity of the profiles, to those shown in Fig 5 for corresponding (higher) values of P ($\approx$ 900 or more). However, interestingly, the profile corresponding to $P = 700$ shows a mixed trend in terms of direction (upward or downward) of the fluid motion in the region under consideration.

As stated earlier, we have also included plots of overall velocity across a

typical cross-section of the circular porous tube by combining q_1, q_2 and q_3 in one graph. These velocity profiles have been shown in Fig 7 (case I) and Fig 8 (case II) for a set of values of P. It is worth noting that the variation of the velocity q_1, corresponding to the bubble region ($0 \leq r \leq 0.3$), shows little, if any, variation with respect to the radial distance in both cases. However, it is seen that there is appreciable variations of velocity in the film ($0.3 \leq r \leq 0.4$) and porous region ($0.4 \leq r \leq 0.5$).

References

[1] G. S. Beavers and D. D. Joseph, Boundary conditions at a naturally permeable wall, J. Fluid Mech., **30** (1967), 197–207.

[2] B. S. Bhatt, The movement of single large liquid bubbles in vertical porous tubes, Rheol. Acta, **22** (1983), 588–591.

[3] B. S. Bhatt and N. C. Sacheti, Flow past a porous spherical shell using the Brinkman model, J. Phys. D, **27** (1994), 37–41.

[4] H. C. Brinkman, A calculation of the viscous force exerted by a flowing fluid on a dense swarm of particles, Appl. Sci. Res. A, **1** (1947), 27–34.

[5] H. C. Brinkman, On the permeability of media consisting of closely packed porous particles, Appl. Sci. Res. A, **1** (1947), 81–86.

[6] A. C. Eringen, Theory of micropolar fluids, J. Math. Mech., **16** (1966), 1–18.

[7] H. L. Goldsmith and S. G. Mason, The movement of single large bubbles in closed vertical tubes, J. Fluid Mech., **14** (1962), 42–58.

[8] H. L. Goldsmith and S. G. Mason, The flow of suspensions through tubes. I. Single spheres, rods and discs, J. Colloid. Sci., **17** (1962), 448–476.

[9] S. Haber and R. Mauri, Boundary conditions for Darcy's flow through porous media, Int. J. Multiphase Flow, **9** (1983), 561–574.

[10] H. Z. Li, X. Frank, D. Funfschilling and P. Diard, Bubbles' rising dynamics in polymeric solutions, Phys. Lett. A, **325** (2004), 43–50.

[11] T. S. Lundgren, Slow flow through stationary random beds and suspensions of spheres, J. Fluid Mech., **51** (1972), 273–299.

[12] G. V. Madhav and R. P. Chhabra, Drag on non-spherical particles in viscous fluids, Int. J. Mineral Process., **43** (1995), 15–29.

[13] H. Power, On the Rallison and Acrivos solution for the deformation and burst of a viscous drop in an extensional flow, J. Fluid Mech., **185** (1987), 547–550.

[14] R. Ravindran, A note on the movement of single large liquid bubbles in vertical tubes, Rheol. Acta, **14** (1975), 693–697.

[15] N. C. Sacheti, Application of Brinkman model in viscous incompressible flow through a porous channel, J. Math. Phys. Sci., **17** (1983), 567–577.

[16] N. C. Sacheti and S. Sampanthar, Viscous flow past a non-Newtonian liquid bubble in vertical permeable tubes: Use of Brinkman model, Proc. Xth Int. Congress Rheology, Sydney, Vol. 2 (1988), 242–244.

[17] S. S. Sadhal and P. S. Ayyaswamy, Flow past a liquid drop with a large non-uniform radial velocity, J. Fluid Mech., **133** (1983), 65–81.

[18] G. F. Tiefenbruck and L. G. Leal, A note on the slow motion of a bubble in a viscoelastic liquid, J. Non-Newtonian Fluid Mech., **7** (1980), 257–264.

[19] A. Tripathi and R. P. Chhabra, Slow motion of a power law liquid drop in another immiscible power law liquid, Arch. Appl. Mech., **62** (1992), 495–504.

[20] C. S. Yih, Dynamics of Non-uniform Fluids, Macmillan, New York (1968).

Received: November 7, 2007

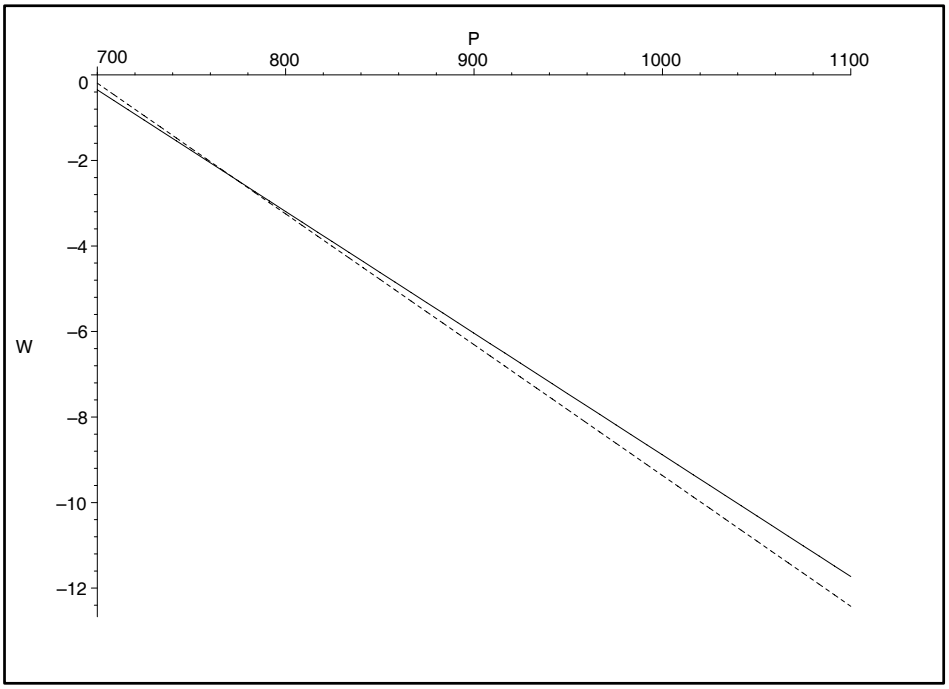

Fig 1. Variation of W with P. $(\rho_1 < \rho_2)$
$k/a^2 = 0.1$ — , $k/a^2 = 0.5$ - - - -

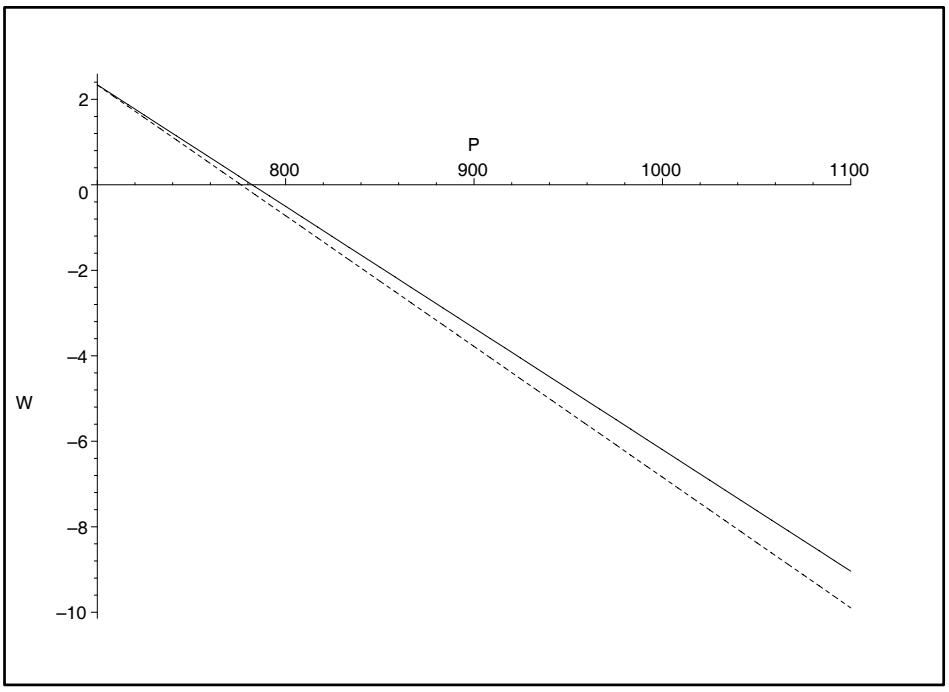

Fig 2. Variation of W with P. $(\rho_1 > \rho_2)$
$k/a^2 = 0.1$ — , $k/a^2 = 0.5$ - - - -

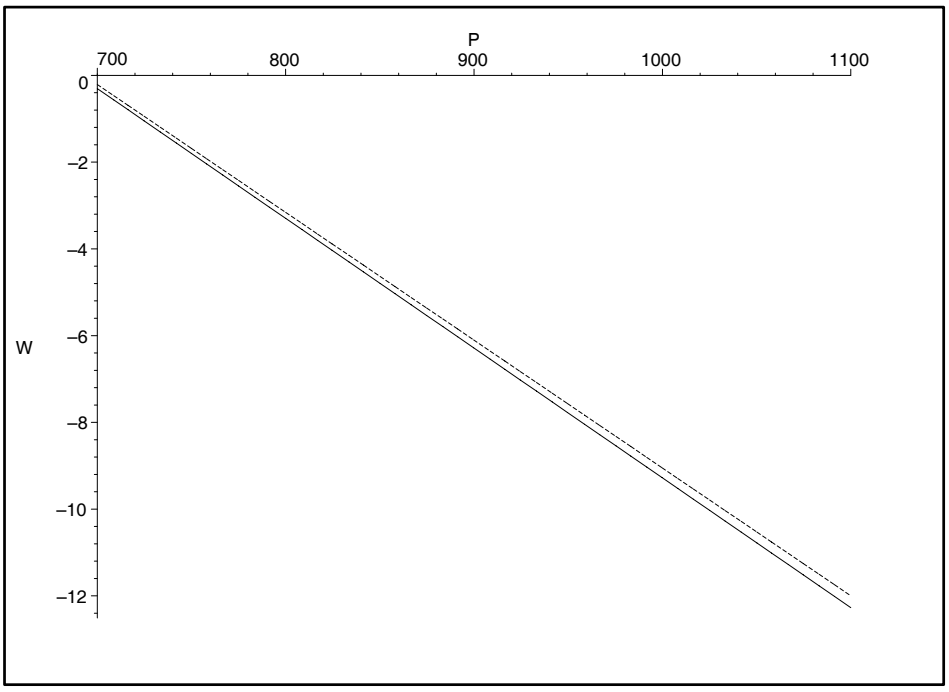

Fig 3. Variation of W with P. $(\rho_1 < \rho_2)$
$m_2/m_1 = 0.1$ — , $m_2/m_1 = 5.0$ - - - -

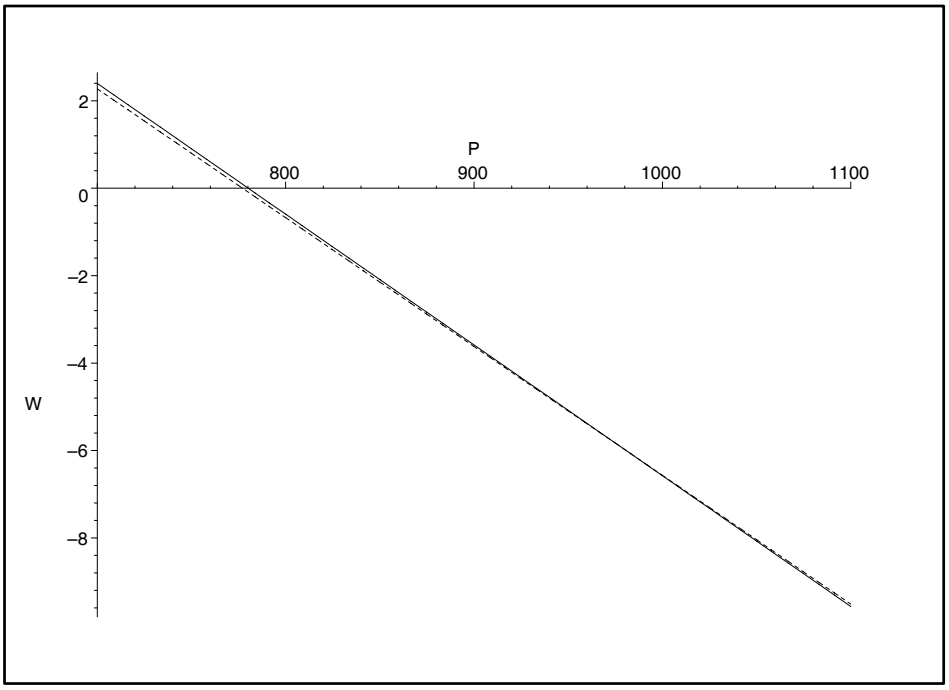

Fig 4. Variation of W with P. $(\rho_1 > \rho_2)$
$m_2/m_1 = 0.1$ — , $m_2/m_1 = 5.0$ - - - -

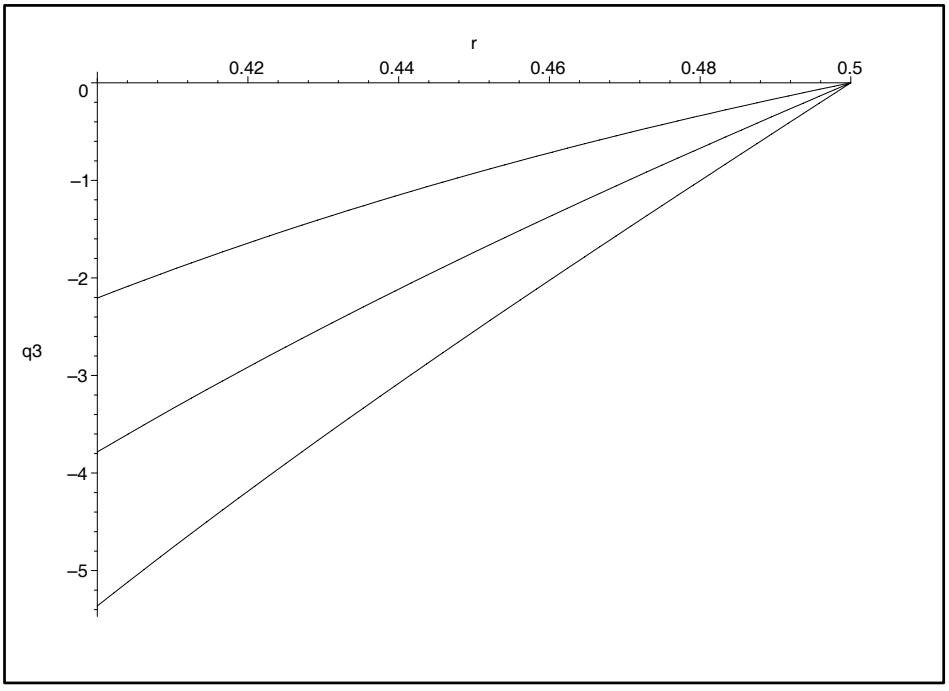

Fig 5. Velocity q_3. $(\rho_1 < \rho_2)$
$P = 900$: top, $P = 1000$: middle, $P = 1100$: bottom

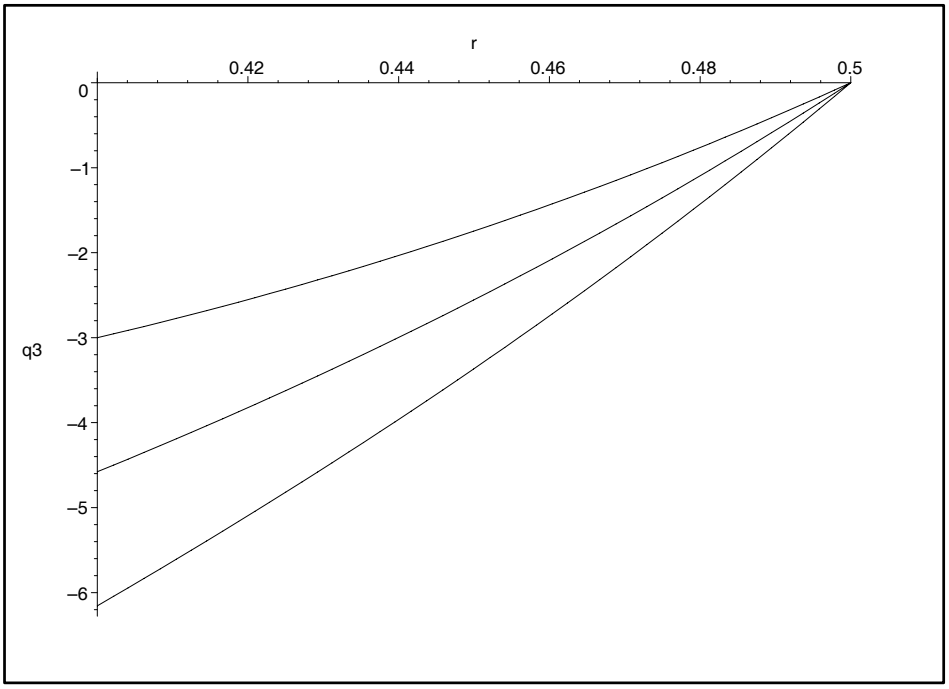

Fig 6. Velocity q_3 . $(\rho_1 > \rho_2)$
$P = 900$: top, $P = 1000$: middle, $P = 1100$: bottom

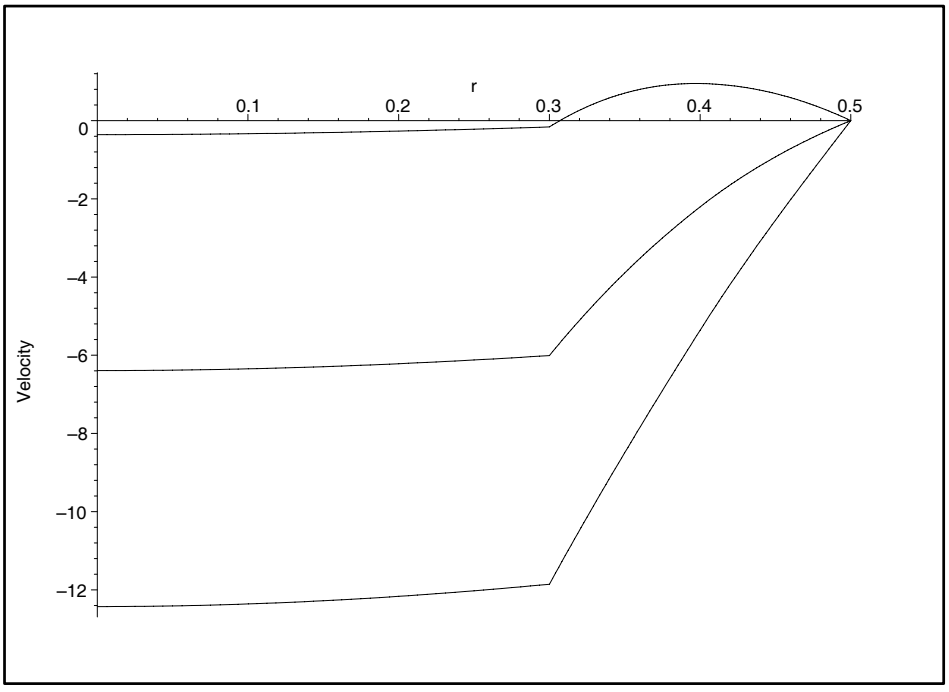

Fig 7. Variation of velocity in different regions. $(\rho_1 < \rho_2)$
$P = 900$: top, $P = 1000$: middle, $P = 1100$: bottom

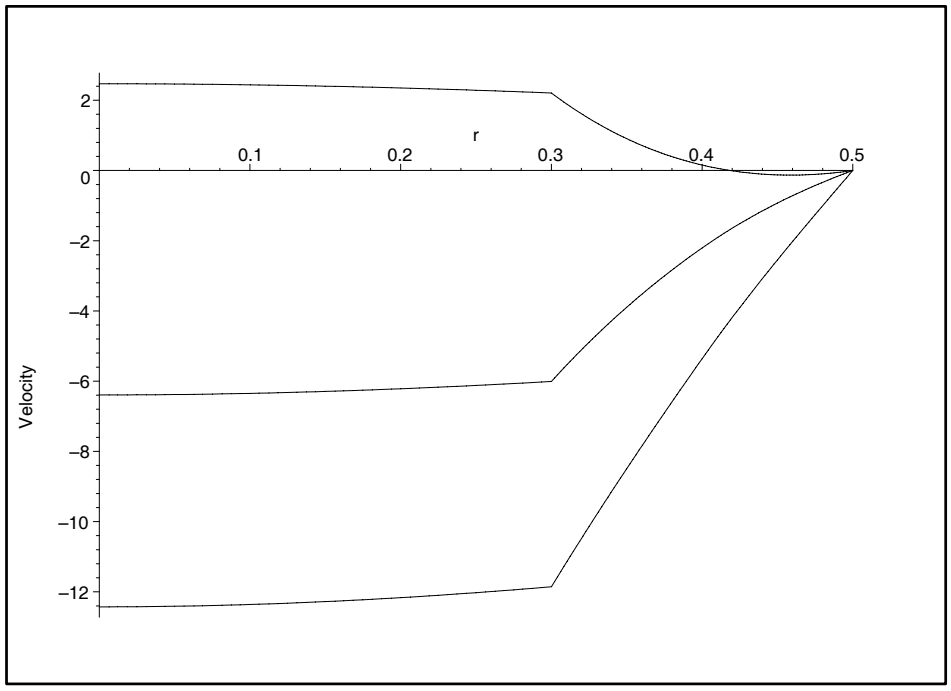

Fig 8. Variation of velocity in different regions. $(\rho_1 > \rho_2)$
$P = 900$: top, $P = 1000$: middle, $P = 1100$: bottom